

Title

Modeling and simulations of methane steam reforming in thermally coupled plate type membrane reactor

Authors

Keyur S. Patel, Aydin K. Sunol

Affiliations

*Department of Chemical Engineering,
University of South Florida,
4202 E. Fowler Avenue,
Tampa,
Florida 33620
USA*

In last decade, interest in cleaner energy technologies such as fuel cells has increased significantly, particularly for power generation and automobile applications. Steam reforming of methane, which has significant potential in fuel cell applications, is also industrially important reaction that is employed in production of ammonia, methanol and in Fischer-Tropsch synthesis (Pena et al., 1996; Furimsky, 1998). In conventional tubular reactor for production of methane from hydrogen, the required heat for reaction is provided indirectly by flue gas flowing in annulus. High endothermicity of reforming reaction and limited wall heat transfer coefficient requires considerable energy input requirement in such reactor (Rostrup-Nielsen, 1984). As opposed to indirect supply of heat by flue gas in conventional tubular reactor, an autothermal reforming of methane combines exothermic oxidation reaction and endothermic reforming reaction in a single reactor (Takeguchi, 2003; Hoang and Chan, 2004). Although autothermal processes are energy efficient, they are not flexible in terms of choice of fuel. In an alternative to autothermal approach, endothermic reaction of steam reforming is coupled with exothermic combustion reaction in such a way that the combustion takes place in the monolith reactor (burner) and the steam reforming takes place in an adjacent channel. Frauhammer et al., (1999) performed interesting simulations and experimental study to couple exothermic and endothermic reactions in a honeycomb monolith reactor. In their study, methane combustion was simulated using palladium coated washcoat. The motivation is to combine energy efficient concept of coupling of an endothermic and exothermic reaction (Frauhammer et al., 1999) and membrane assisted selective separation of hydrogen in a single reactor in order to produce pure hydrogen.

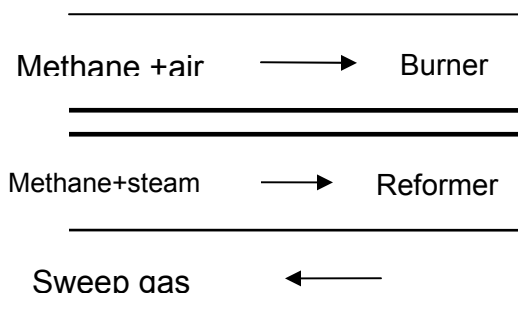


Fig. 1. Schematic diagram of the reactor

As shown in a schematic diagram (Fig. 1.), the reactor is composed of three channels. Methane combustion takes place in the first channel on $\text{Pt}/\delta\text{-Al}_2\text{O}_3$ catalyst supplying the required heat for endothermic steam reforming. Methane steam reforming takes place in second channel on $\text{Ni}/\text{MgO}-\text{Al}_2\text{O}_3$ catalyst. Both the reformer and the combustion catalyst form thin layers on both sides of the reactor wall that decreases the heat transfer resistance significantly as indicated by thick shaded lines in Fig. 1. Selective permeation of hydrogen through palladium membrane is achieved by counter-current flow of sweep gas through the third channel. As shown in Fig. 1, flow through the reformer and the burner is co-current while that through the sweep gas and the reformer gas is counter-current. Both burner and reformer channels are modeled as monolith reactors. The temperature and composition dependence of viscosity and diffusivity of the burner and the reformer gas mixture is incorporated in the

model. Both the homogenous and catalytic combustion of methane is considered in the model. Axial diffusion of heat and mass in the fuel gas, the reformer gas and the catalyst layers is neglected. Pressure inside both the burner and the reformer is assumed to be constant. Conduction and convection are assumed to be predominant heat transfer mechanism while radiation effect is neglected. Heat loss to surrounding is neglected and both the process gas and the fuel gas are treated as an ideal gas.

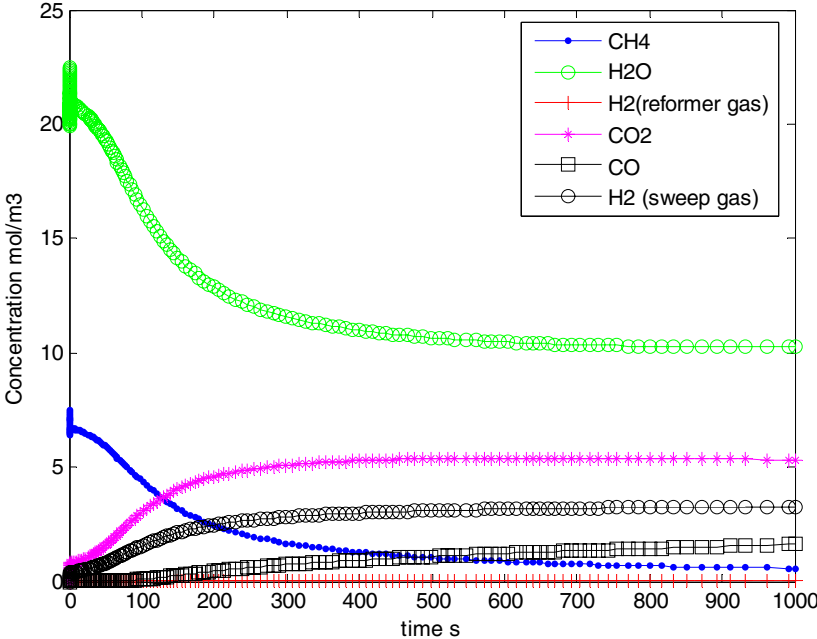
The material and energy balance equations result in a set of 25 partial differential equations which are discretized using orthogonal spline collocation on finite elements (Boor, 1978). The reactor length is divided into 9 intervals with 3 collocation points in each interval. Discretized partial differential equations along with boundary conditions form system of stiff differential algebraic equations which are solved using stiff integrator that utilizes variable order solver based on numerical differentiation formulas. The computations are performed using MATLAB programming environment. Effects of various operating conditions like steam/methane ratio, inlet gas temperatures, gas inlet velocities and sweep gas flow rate are investigated by numerical simulations. From results, reactor performance is analyzed based on methane conversion, hydrogen recovery yield and maximum wall temperature for above stated operating conditions. Simulations are also performed for the co-current flow mode of the sweep gas to compare the hydrogen recovery yield for two different flow modes.

Dynamic and steady state simulations for the base case

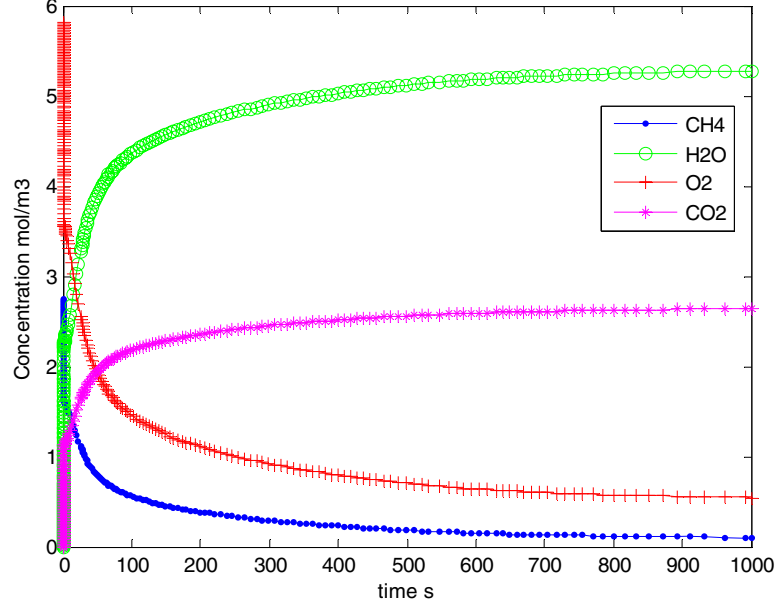
Results for only base case simulations are presented and discussed here. Fig. 2(a) and Fig. 2(b) show concentration profiles of the reformer product gas, the burner product gas and the outlet sweep gas vs. time. Profiles indicate that reactor reach steady state in about 800s. The dynamic simulations are followed by the steady state simulations. Temperature profiles obtained from the steady state simulations are shown in Fig. 3(a). As shown in Fig. 3(a), reactor wall temperature reaches a maximum at an initial section of the reactor and then decreases along the length. Reformer gas temperature first increases due to higher wall temperatures and then decreases as it flows along reactor due to countercurrent heat transfer with relatively cold sweep gas. Sweep gas temperature increases along the reactor length due to heat transfer with reformer gas. As burner and reformer product gas approach reactor end, reactor wall temperature decreases due to lower reformer gas temperature and low fuel conversion. Steady state and dynamic simulations also reveals that burner catalyst, reformer catalyst and reactor wall temperatures show same profiles along the reactor length due to much lower heat transfer resistance between them.

Figs. 2(e) and (f) depict dynamic and steady state concentration profiles of hydrogen in reformer gas and sweep gas respectively. Profiles show that concentration of hydrogen in reformer gas first increases and then decreases along the reactor length while hydrogen concentration in sweep gas increases continuously till an initial section of the reactor and then decreases very little. This means that due to higher catalyst temperature initially, the reforming rate is higher than the permeation rate. As the reactor wall temperature falls and the hydrogen partial pressure increases along reactor length, permeation becomes more dominant than

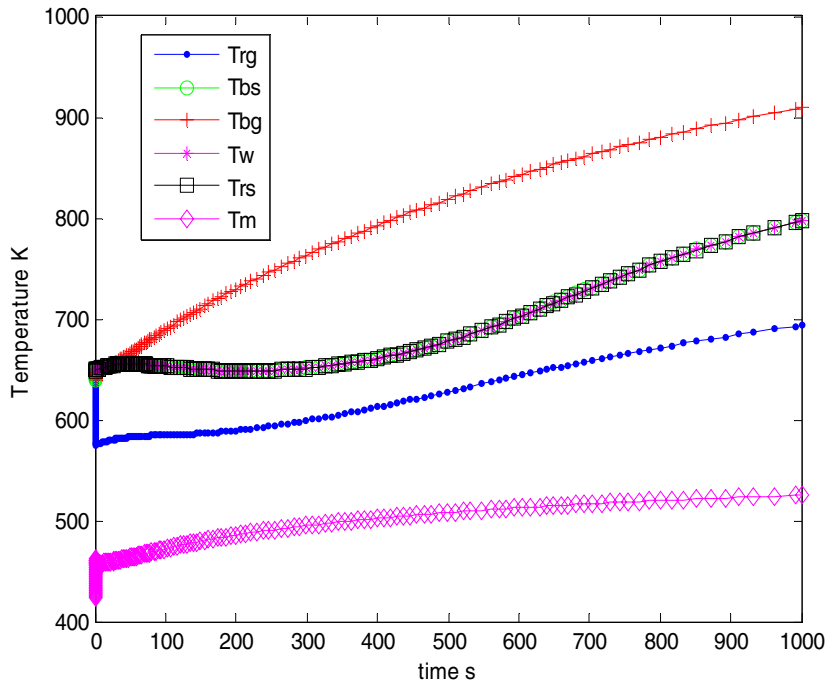
reforming. Little decrease in concentration of hydrogen in sweep gas at reactor entrance explains occurrence of reverse permeation of hydrogen due to high partial pressure of hydrogen in sweep gas. As indicated in steady state concentration profiles (see Fig. 3(b)), carbon monoxide concentration first increases and then decreases along length of reactor. For base case configuration, methane conversion of 92.33% and hydrogen recovery yield of 86.94 % is obtained with maximum wall temperature reaching 1360.5 K and carbon monoxide concentration approaching 1.6153 mol/m^3 .



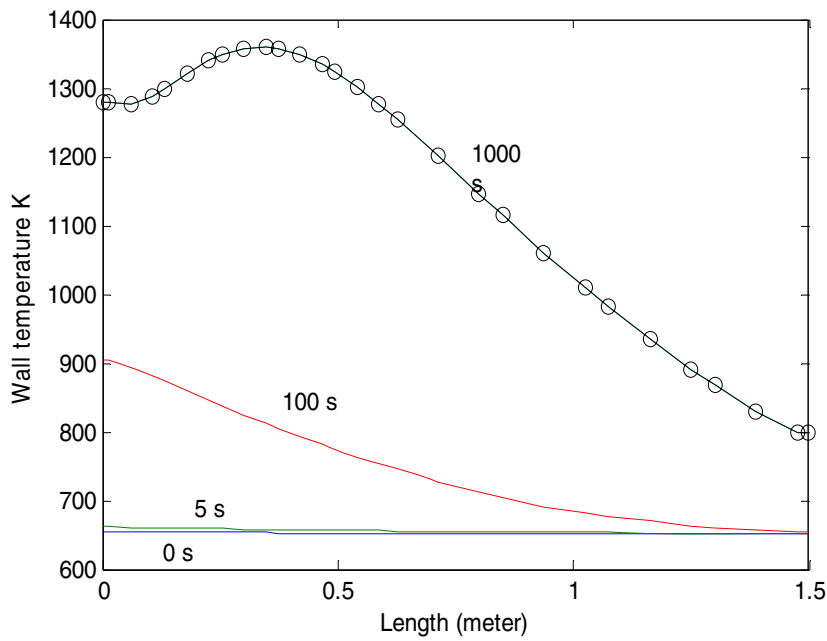
(a)



(b)



(c)



(d)

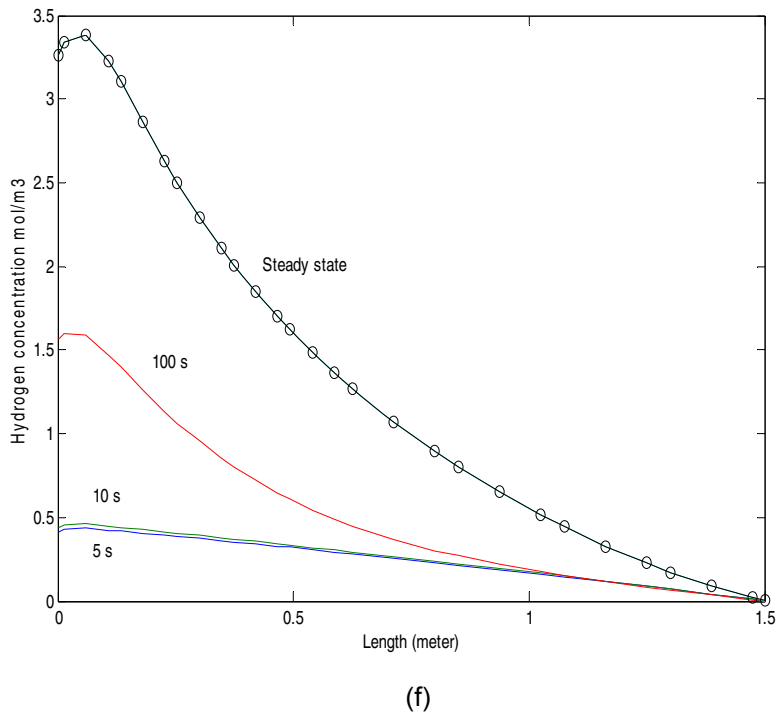
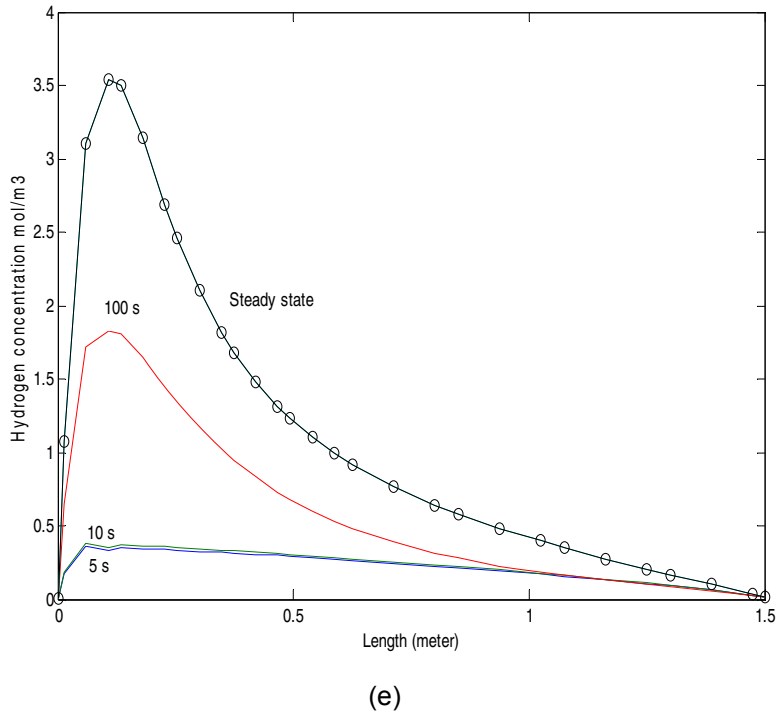


Fig. 2. Dynamic behavior of (a) reformer product gas concentration, (b) burner product gas concentration, (c) reformer and burner product gas temperatures, (d) wall temperature profile, (e) hydrogen concentration profile in reformer gas and (f) hydrogen concentration profile in sweep gas for the base case.

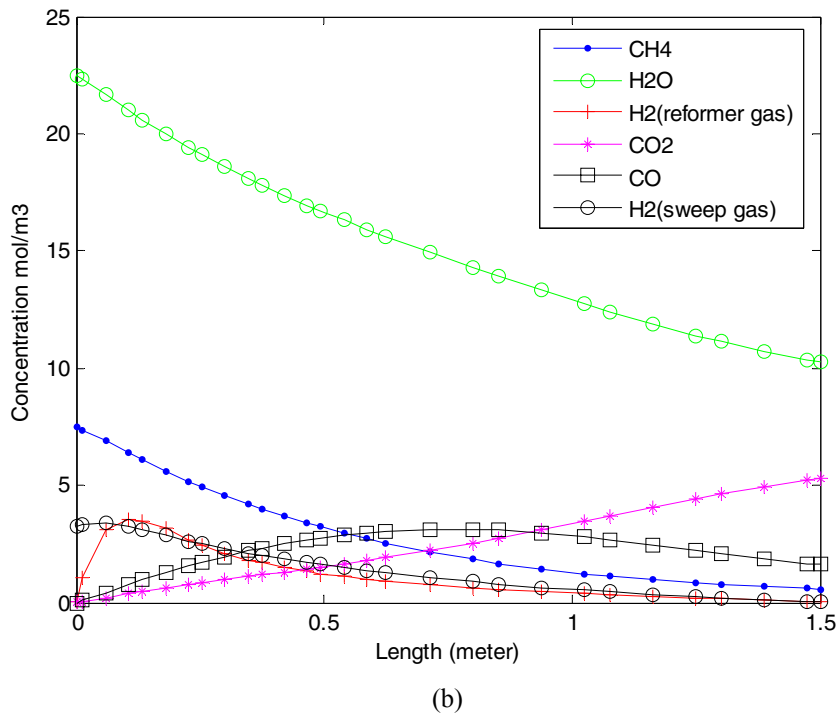
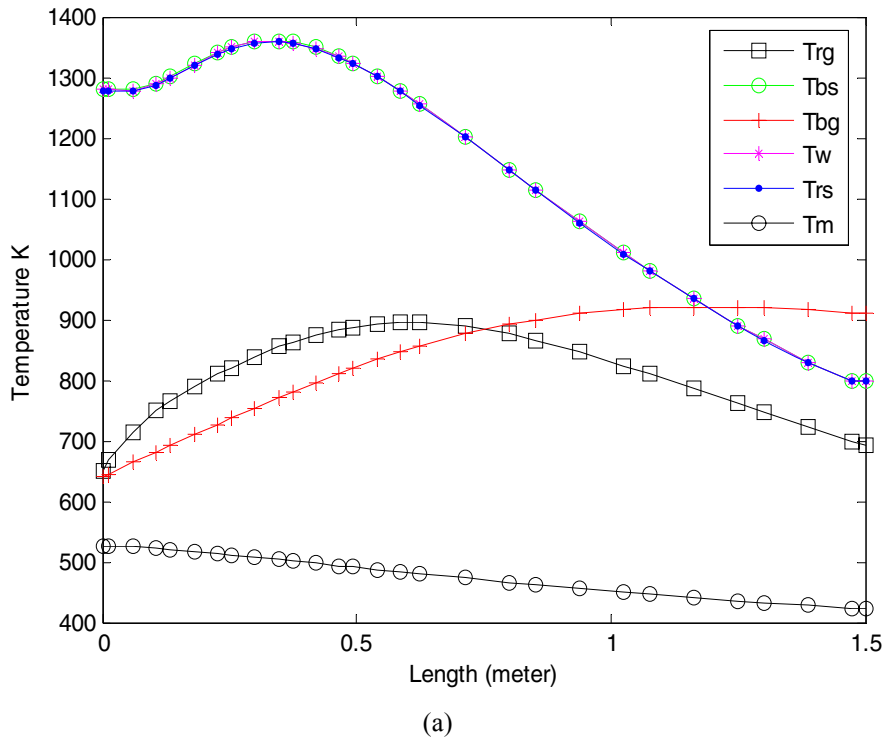


Fig. 3. Steady state behavior for the base case (a) temperature profiles; (b) concentration profiles.

As stated earlier, dynamic and steady state simulations are carried out for different operating conditions like inlet fuel concentration, steam to methane ratio, sweep gas flow rate, inlet reformer gas temperature and inlet gas velocities. From results, the reactor performance is evaluated based on methane conversion, hydrogen recovery yield and maximum wall temperature. Simulations are also performed for co-current mode of sweep gas flow for comparison. Results show that introduction of membrane reactors can enhance hydrogen recovery yield in such a reactor. Reactor performance is found to be very sensitive to operating decisions like fuel concentration, inlet reformer and burner gas velocities and inlet reformer gas temperature. Countercurrent operation of sweep gas increases hydrogen recovery yield compared to co-current operation, with proper selection of sweep gas flow rate. At constant pressure, increase in steam/methane ratio, fuel concentration, burner gas velocity or inlet reformer gas temperature leads to higher wall temperatures, higher methane conversion and higher hydrogen recovery yield. Decrease in reformer inlet gas velocity reduces maximum wall temperature for constant pressures resulting in lower methane conversion and lower hydrogen recovery yield.

References

Boor, C. D., 1978. A Practical Guide to Splines. Springer-Verlag, New-York.

Frauhammer, J., Eigenberger, G., Hippel, L. V., Arntz, D., 1999. A new reactor concept for endothermic high-temperature reactions. Chemical Engineering Science 54, 3661-3670.

Furimsky, E., 1998. Selection of catalysts and reactors for hydroprocessing. Applied Catalysis A 171, 177-206.

Hoang, D. L., Chan, D. L., 2004. Modeling of a catalytic autothermal methane reformer for fuel cell applications. Applied Catalysis A: General 268, 207-216.

Pena, M. A., Gomez, J. P., Fierro, J. L. G., 1996. New catalytic routes for syngas and hydrogen production. Applied Catalysis A 144, 7-57.

Rostrup-Nielsen, J. R., 1984. In J. R. Anderson & M. Boudart Eds. Catalysis, science and technology, Catalytic steam reforming vol. 5. Berlin, Springer.

Takeguchi, T., Furukawa, S. N., Inoue, M., Eguchi, K., 2003. Autothermal reforming of methane over Ni catalyst supported over CaO-CeO₂-ZrO₂ solid solution. Applied Catalysis A: General 240, 223-233.